Soft and Hard Molecule-Based Magnets of Formula $[(Etrad)_2M_2\{Cu(opba)\}_3]\cdot S$ [$Etrad^+$ = Radical Cation, M^{II} = Mn^{II} or Co^{II}, opba = *Ortho*-phenylenebis(oxamato), S = Solvent Molecules], with a Fully Interlocked Structure

Maria G. F. Vaz,[b] Luiza M. M. Pinheiro,[b] H. O. Stumpf,*[b] Antônio F. C. Alcântara,[c] Stéphane Golhen,[d] Lahcène Ouahab,[d] Olivier Cador,[a] Corine Mathonière,[a] and Olivier Kahn*[a]

Abstract: The goal of this work was to explore the chemistry and the physics of a family of molecule-based magnets containing three spin carriers, with a fully interlocked structure. The main emphasis was on the coercivity of these magnets, which confers a memory effect on the materials. For this, three compounds have been synthetized, namely the precursor $[(Etrad)_2Cu(opba)]\cdot CH_3CN\cdot H_2O$ (**1**), and the magnets $[(Etrad)_2Mn_2\{Cu(opba)\}_3(DMSO)_{0.5}]\cdot 0.25\,H_2O$ (**2**) and $[(Etrad)_2Co_2\{Cu(opba)\}_3(DMSO)_{1.5}]\cdot 0.25\,H_2O$ (**3**), where $Etrad^+$ stands for the radical cation 2-(1-ethylpyridinium-4-yl)-4,4,5,5-tetramethylimidazolin-1-oxyl-3-oxide, and opba stands for *ortho*-phenylenebis(oxamato). The crystal structures of the three compounds have been determined. The structure of **1** consists of planar Cu(opba) units with one of the radical cations weakly bound to the Cu^{2+} ion, the other radical cation being rather isolated. Compounds **2** and **3** are isomorphous. Their structure consists of two interpenetrating graphitelike networks with edge-sharing hexagons. The magnetic properties of the three compounds have been investigated in detail. For compounds **2** and **3** the temperature dependences of the direct current (dc) and alternating current (ac) magnetic responses have been measured along with the field dependence of the magnetization. Both compounds exhibit a long-range magnetic ordering with a spontaneous magnetization. The critical temperatures are 22.8 K and 37 K for **2** and **3**, respectively. While **2** is a soft magnet, **3** has been found to be a very hard magnet, with a coercive field depending on the particle size. This coercive field may reach 24 kOe at 6 K for a sample consisting of very small crystals. Mixed materials with the abbreviated formula $[Etrad_2Mn_{2-2x}Co_{2x}Cu_3]$ (**4** – *x*) have also been synthesized. Their critical temperatures have been found to vary almost linearly with *x*. The *x* dependence of the coercive field has also been investigated and analyzed.

Keywords: catenanes · magnetic properties · magnets · supramolecular chemistry

Introduction

Since the discovery of the first molecule-based magnets,[1–4] a large number of molecule-based materials exhibiting a spontaneous magnetization below a critical temperature T_c have been reported.[5–10] In many cases these compounds contain two kinds of spin carriers, either two different metal ions,[11–15] or a metal ion and an organic radical.[16–25] Today different topologies are known, ranging from quasi one-dimensional systems with small T_c values to three-dimensional networks with T_c values higher than room temperature. One of the challenges for a chemist in this field of research is to control the topology in order to obtain interactions between spin carriers in the three directions of the space. To build a three-dimentional network, a specific type of building block or brick is necessary. The hexacyanometallates, $[M(CN)_6]^{3-}$, are certainly the best known examples of building blocks capable of giving infinite linkages along three perpendicular directions.[26–29] The trisoxalatometallates,

[a] Prof. O. Kahn, O. Cador, C. Mathonière
Laboratoire des Sciences Moléculaires
Institut de Chimie de la Matière Condensée de Bordeaux
UPR CNRS No 9048, 33608 Pessac (France)
Fax: (+33) 56-84-26-49
E-mail: kahn@icmcb.u-bordeaux.fr

[b] Prof. H. O. Stumpf, M. G. F. Vaz, L. M. M. Pinheiro
Departamento de Química, ICEx
Universidade Federal de Minas Gerais
Belo Horizonte, MG 31.270-901 (Brazil)
Fax: (+55) 314995700
E-mail: stumpf@dedalus.lcc.ufmg.br

[c] A. F. C. Alcântara
Departamento de Química, ICE
Fundação Universidade do Amazonas
Manaus, AM 69.078-000 (Brazil)

[d] S. Golhen, L. Ouahab
Laboratoire de Chimie du Solide et Inorganique Moléculaire
UMR CNRS No 6511, Université de Rennes 1, 35042 Rennes (France)

0947-6539/99/0505-1486 $ 17.50+.50/0 *Chem. Eur. J.* **1999**, *5*, No. 5

$[M(C_2O_4)_3]^{3-}$, may also lead to three-dimensional networks. However, it is then necessary to control the chirality of the M sites, which all have to be identical. Few examples of such chiral three-dimensional networks are known; their critical temperatures, if any, are below 10 K.[30, 31] Most often, the M sites adopt the two conformations, Λ and Δ, in equal proportions, and the structure consists of two-dimensional honeycomblike networks. Many compounds of that kind have been reported in the last few years.[12, 32–34]

In 1993 we reported on a compound whose structure consisted not of one but two interpenetrating quasi-perpendicular honeycomblike networks.[36, 37] Its formula is $[(Merad)_2Mn_2\{Cu(opba)\}_3(DMSO)_2]\cdot 2H_2O$, in which Merad stands for 2-(1-methylpyridinium-4-yl)-4,4,5,5-tetramethylimidazolin-1-oxyl-3-oxide and opba for *ortho*-phenylenebis(oxamato). This compound behaves as a soft magnet below 22.5 K. To explore all the potentialities arising from this peculiar topology, we made efforts to synthesize and characterize structurally other fully interlocked compounds. Our main concern was the design of hard magnets retaining the peculiar and aesthetic structure of $[(Merad)_2Mn_2\{Cu(opba)\}_3(DMSO)_2]\cdot 2H_2O$. The coercivity is indeed one of the main characteristics of a magnet; it confers the memory effect. We also wanted to compare the physical properties of soft and hard magnets with the same structure. In this paper we report on our latest findings. We first describe the syntheses and the structures of the precursor $[(Etrad)_2Cu(opba)]\cdot CH_3CN\cdot H_2O$ (**1**), in which $Etrad^+$ stands for 2-(1-ethylpyridinium-4-yl)-4,4,5,5-tetramethylimidazolin-1-oxyl-3-oxide, and of the bimetallic compounds $[(Etrad)_2Mn_2\{Cu(opba)\}_3(DMSO)_{0.5}]\cdot 0.25H_2O$ (**2**) and $[(Etrad)_2Co_2\{Cu(opba)\}_3(DMSO)_{1.5}]\cdot 0.25H_2O$ (**3**). Then, we investigate the magnetic properties of the three compounds in great detail, with a specific emphasis on the critical temperature and coercive field values. As expected **2** and **3** are molecule-based magnets, with $T_c = 22.8$ K and 37 K, respectively. While **2** behaves as a soft magnet, **3** exhibits an exceptionally strong coercivity, as compared with other magnetic molecular materials. Finally, we demonstrate that it is possible to fine-tune the critical temperature and the coercivity in this class of materials by synthesising mixed compounds of abbreviated formula $Etrad_2Mn_{2-2x}Co_{2x}Cu_3$.

Editorial Board Member:[*] *Oliver Kahn is a Graduate Engineer in Chemistry. He received his Ph.D. degree from the University of Paris in 1969. He became Professor in Chemistry at the University of Paris South in 1975, where he founded and directed the Laboratoire de Chimie Inorganique. In 1995, he moved to the Insititut de Chimie de la Matière Condensée de Bordeaux (ICMCB), where he founded the Laboratoire des Sciences Moléculaires. He is currently Professor at the Universtiy of Bordeaux I, and a Member of the Institut Universitaire de France. Olivier Kahn is a Member of the (French) Academy of Science. His fields of resarch are molecular materials, molecular electronics, and molecular magnetism. He has already published some 300 research papers, along with seven books, including Molecular Magnetism in 1993.*

[*] Members of the Editorial Board will be introduced to readers with their first manuscript.

Results

Description of the structures

*Compound **1***: The structure of the precursor (**1**) is shown in Figure 1. It consists of mononuclear $Cu(opba)^{2-}$ units, two kinds of radical cations, and noncoordinated CH_3CN and H_2O molecules (Figure 1). One of the radical cations is very weakly

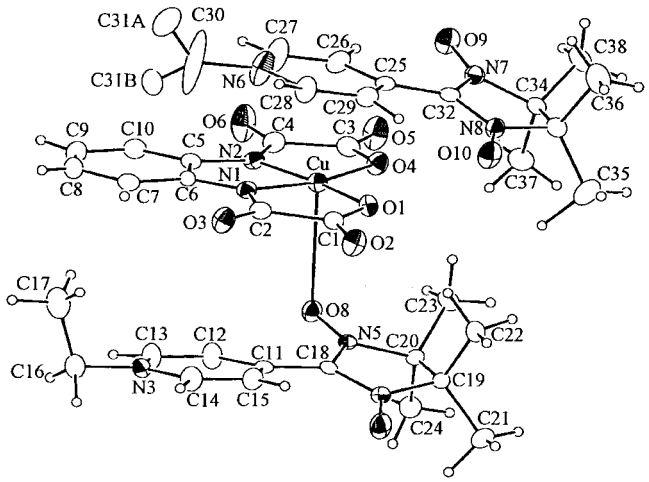

Figure 1. View of the precursor **1**. For the sake of simplicity, the noncoordinated solvent molecules have been omitted.

bound to the copper atom of the anion, and the other is rather isolated. The copper atom is in a square-pyramidal environment, with two nitrogen and two oxygen atoms from the oxamato groups in the basal plane and an oxygen atom from the former radical cation in the apical position. The average values of the Cu–N and Cu–O bond lengths in the basal plane are 1.89 Å and 1.95 Å, respectively, and the Cu–O apical bond length is 2.834(5) Å. The corresponding bond angle Cu-O-N is 111.4(3)°. The shortest intermolecular contact involving the isolated radical cation is found between a hydrogen atom of the pyridinium ring and an oxamato oxygen atom. This H–O separation is equal to 2.015 Å.

*Compounds **2** and **3***: The compounds **2** and **3** are isomorphous and their structure is similar to that described for $[(Merad)_2Mn_2\{Cu(opba)\}_3(DMSO)_2]\cdot 2H_2O$.[37] The general architecture consists of two equivalent two-dimensional networks denoted A and B. Each network is formed by parallel honeycomb layers. A layer is made up of edge-sharing hexagons with M^{2+} ions (M = Mn or Co) at each corner and Cu^{2+} ions at the middle of each edge, as shown in Figure 2. Two nearest neighbor metal ions are bridged by an oxamato group. Structural information concerning the hexagons is

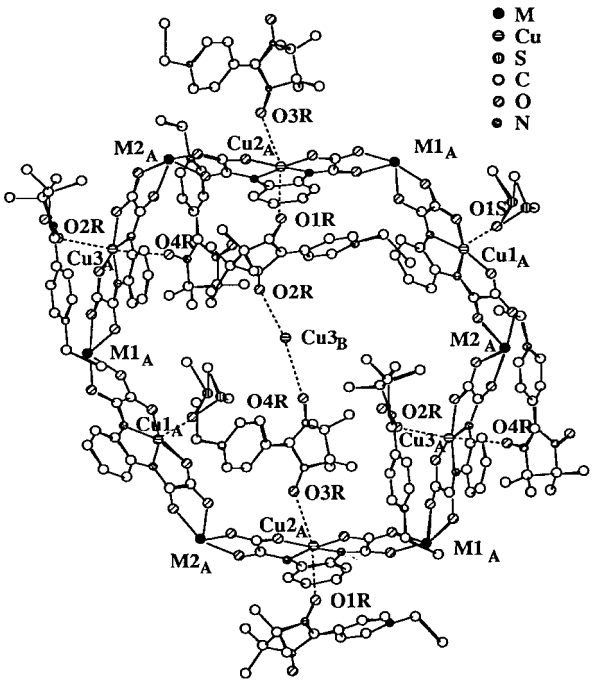

Figure 2. View of a hexagon A in compounds **2** (M = Mn) and **3** (M = Co) along with the copper atom belonging to hexagon B, located nearby the center of hexagon A. This view also shows the presence of $Cu2_A$-Etrad-$Cu3_B$ chains connecting the A and B networks.

given in Table 1. The layers of each network stack above each other in a graphitelike fashion. The mean interlayer separation is 14.68 Å for **2** and 14.82 Å for **3**.

Table 1. Structural information on the hexagons M_6Cu_6 (M = Mn and Co) for compounds **2** and **3**. All distances [Å] are mean distances.

	2	**3**
edge length (distance between corners)	10.62	10.47
M–Cu distance along an edge	5.37	5.28
distances between opposite corners	21.09	20.85
bond lengths around metal ions:		
M–O	2.13	2.09
Cu–O	1.97	1.97
Cu–N	1.92	1.92

The A and B networks interpenetrate with a full interlocking of the M_6Cu_6 hexagons, as shown in Figure 3 (the radical cations and solvent molecules were omitted for clarity). These networks make dihedral angles of 71.8° for **2** and 73.2° for **3**; these are smaller than that found for $[(Merad)_2Mn_2\{Cu(opba)\}_3(DMSO)_2]\cdot 2H_2O$ (83.4°). The topology may be described as a three-dimensional wire netting. The hexagons are connected further through radical cations that bridge two copper atoms, one belonging to the network A, the other one to the network B. More precisely, a copper atom Cu3 (Cu2) is located very nearby the center of a hexagon belonging to network A (B), and is bound to two other copper atoms Cu2 (Cu3) by radical cations which play the role of bridging units between the two networks. The resulting chains $Cu2_A$-Etrad-$Cu3_B$ ($Cu3_A$-Etrad-$Cu2_B$) define two directions making dihedral angles of 71.8° for **2** and 73.2°

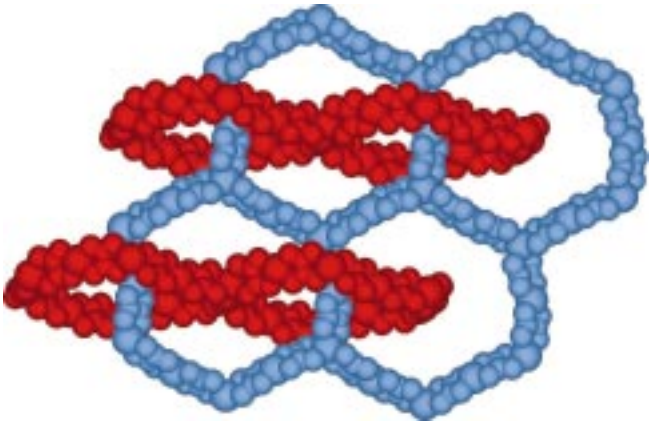

Figure 3. Interpenetration and interlocking of the networks A and B in compounds **2** and **3**.

for **3**, and the intrachain separations are 8.512(6) Å (10.327(6) Å) for **2** and 8.648(7) Å (9.917(7) Å) for **3**.

Let us now describe the surroundings of the metal centers. There are three crystallographically independent Cu(opba) groups, and within each hexagon two crystallographically equivalent copper atoms are opposite to each other. Each copper atom has a square-based coordination with two nitrogen and two oxygen atoms arising from two oxamato groups. The average values of Cu–N and Cu–O bond lengths are reported in Table 1. Cu1 is bound to one DMSO molecule with a Cu1–O apical bond length of 2.26(3) Å in **2** and 2.17(3) Å in **3** (the additional DMSO molecule in **3** is not coordinated). Both Cu2 and Cu3 are bonded to two radical cations through oxygen atoms. The related Cu–O bond lengths are given in Table 2. The deviations with respect to

Table 2. Apical distances [Å] around the copper atoms for compounds **2** and **3**.

	2	**3**
Cu1–O1S	2.26 (3)	2.17(3)
Cu2–O1R	2.813(24)	2.798(27)
Cu2–O3R	2.970(30)	2.846(30)
Cu3–O2R	2.629(21)	2.699(23)
Cu3–O4R	3.135(25)	2.938(37)

the mean plane defined by the oxamato atoms N2O2 are larger for Cu1 (0.182 Å in **2** and 0.200 Å in **3**) than for Cu2 and Cu3 (< 0.1 Å). Two crystallographically independent manganese or cobalt atoms noted M1 and M2 occupy two chiral sites. Each M atom is bonded to six oxygen atoms arising from three oxamato groups. The three copper atoms that are bridged to an M atom through oxamato groups are crystallographically independent. The structure presents a perfect alternation of Λ and Δ chiral sites (Figure 4).

Finally, there are two crystallographically independent radical cations. The dihedral angles between the pyridinium ring and the mean plane of the five-membered imidazoline-1-oxyl-3-oxide ring are equal to 27.09° and 17.50° in **2** and 27.03° and 21.59° in **3**.

At the end of this structural section, it is worth mentioning that a general presentation of interlocked structures has recently appeared.[38]

0947-6539/99/0505-1488 $ 17.50+.50/0 *Chem. Eur. J.* **1999**, *5*, No. 5

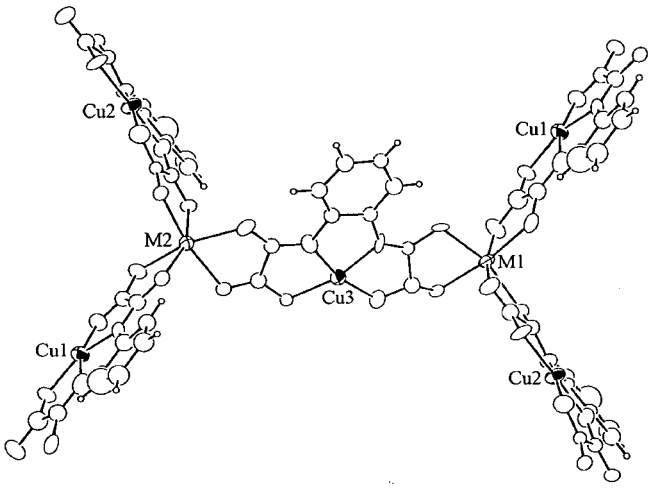

Figure 4. Edge of a hexagon in compounds **2** and **3** showing the Λ and Δ chiral sites M^{2+} bridged by the Cu(opba) unit.

Magnetic properties

*Compound **1***: The magnetic susceptibility data for **1** are shown in Figure 5 in the form of the $\chi_M T$ versus T curve; χ_M is the molar magnetic susceptibility and T the temperature. At room temperature $\chi_M T$ is equal to 0.98 emu K mol^{-1}. As T is lowered, $\chi_M T$ first increases, reaches a maximum at 9.8 K, with $\chi_M T = 1.38$ emu K mol^{-1}, and then decreases. The profile of this $\chi_M T$ versus T curve indicates that some ferromagnetic interactions are operative.

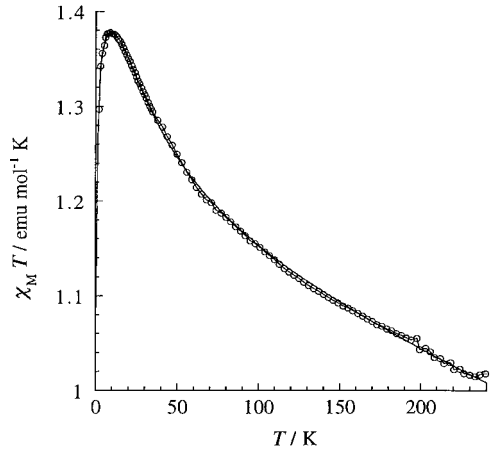

Figure 5. Experimental (—) and calculated (○) $\chi_M T$ versus T plots for compound **1**.

These magnetic susceptibility data may be interpreted by considering a ferromagnetically coupled [(Etrad)Cu(opba)]$^-$ heterospin pair together with an isolated radical cation. The zero-field Hamiltonian for the pair is given in Equation (1), in which J_{CuRad1} is the singlet–triplet energy gap. The theoretical expression of $\chi_M T$ is then given by Equation (2),

$$H = -J_{CuRad1} S_{Cu} \cdot S_{Rad1} \quad (1)$$

$$\chi_M T = \frac{2N\beta^2 g^2}{k} \frac{1}{3 + \exp(-J_{CuRad1}/kT) - 2zJ'/kT} + \frac{N\beta^2 g^2}{3k} S_{Rad2}(S_{Rad2}+1) + \chi_{dia} T \quad (2)$$

in which the first term in the right-hand side concerns the pair, the second term concerns the isolated radical cation, and the third term is the core diamagnetism.

In Equation (2) the local Zeeman factors were assumed to be equal and isotropic. The decrease of $\chi_M T$ in the low-temperature range may be attributed to intermolecular interactions, which were accounted for in the mean-field approximation. zJ' stands for the intermolecular interaction parameter. Least-squares fitting of the experimental data led to $J_{CuRad1} = 31$ cm^{-1}, $g = 2.04$, $zJ' = -0.25$, and $\chi_{dia} = -742 \times 10^{-6}$ emu mol^{-1}. The agreement factor R defined by $\Sigma[(\chi_M T)^{obs} - (\chi_M T)^{cal}]^2/\Sigma[(\chi_M T)^{obs}]^2$ was then found to be 3.0×10^{-4}. One will notice that the core diamagnetism is substantially larger than the value calculated from the Pascal tables. Such a situation was already found in some other compounds involving organic radicals. The important point is that the interaction between the Cu^{2+} ion and the radical cation bound to it is significantly ferromagnetic. Gatteschi and co-workers already showed that the interaction between a Cu^{2+} ion and a nitronyl nitroxide radical occupying an apical position may be ferromagnetic.[23]

*Compound **2***: Both the temperature and field dependences of the direct current (dc) magnetic response along with the temperature dependence of the alternating current (ac) magnetic response were investigated. The $\chi_M T$ versus T plot shown in Figure 6 is characteristic of ferrimagnetic compounds of the formula $[(cat)_2Mn_2\{Cu(opba)\}_3] \cdot S$.[35] At room temperature $\chi_M T$ is equal to 8.26 emu K mol^{-1}, which is slightly

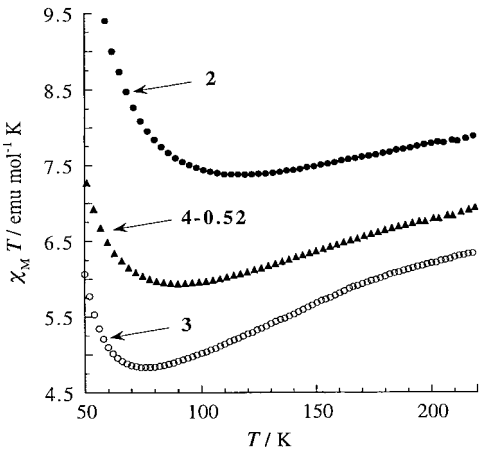

Figure 6. $\chi_M T$ versus T plots for compounds **2**, **3**, and **4 – 0.52**.

lower than expected for isolated spin carriers. As T is lowered, $\chi_M T$ first decreases smoothly, reaches a rounded minimum around 120 K, and then increases very abruptly before reaching a maximum around 20 K. The minimum in the $\chi_M T$ versus T plot reveals antiferromagnetic interactions between nearest-neighbor Mn^{2+} and Cu^{2+} ions without correlation length, and the huge increase of $\chi_M T$ at low temperature is due to the increase of the correlation length with the $S_{Mn} = 5/2$ spins aligned along the field direction and the $S_{Cu} = 1/2$ spins aligned along the opposite direction. There is no theoretical model to quantitatively interpret these magnetic data because

of the complexity of the structure as well as the presence of three kinds of spin carriers. The $\chi_M T$ versus T curve for **2** is very close to that observed for $[(NBu_4)_2Mn_2\{Cu(opba)\}_3]\cdot S$.[35] In particular, the minima of $\chi_M T$, characteristic of the ferrimagnetic regime, occur at the same temperature. From this $\chi_M T$ curve it is not possible to determine the specific behavior of the radical-cation spins. However, the field dependence of the magnetization for $[(Merad)_2Mn_2\{Cu(opba)\}_3(DMSO)_2]\cdot 2H_2O$ up to 200 kOe has confirmed that the radical cation interacts ferromagnetically with the Cu^{2+} ion to which it is bound. It follows that the radical spins tend to align along a direction opposite to that of the S_{Mn} spins.[37]

The χ_M versus T plot shows a break around 23 K corresponding to a long-range magnetic ordering. To fully characterize this magnetically ordered state, the temperature dependences of the field-cooled magnetization (FCM), the remnant magnetization (REM), and the in-phase and out-of-phase ac susceptibilities (at a frequency of 125 Hz and a drive amplitude of 3 Oe), χ_M' and χ_M'', were measured. The results are displayed in Figure 7. The FCM curve shows a very rapid

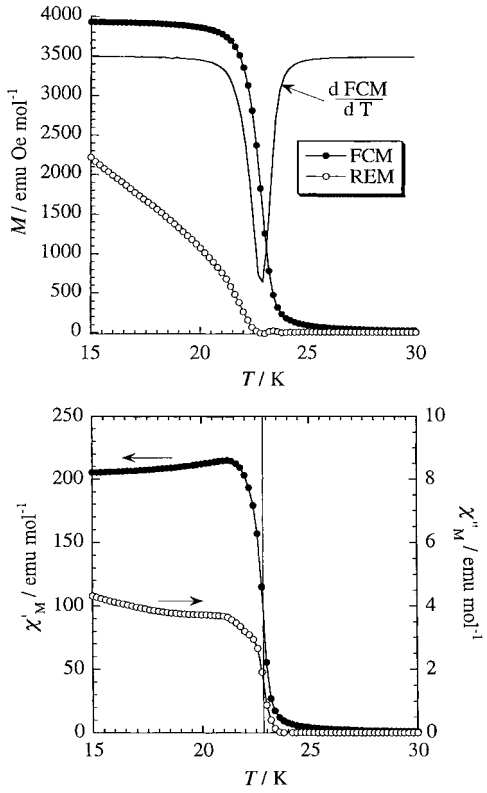

Figure 7. Top: FCM and REM versus T curves for compound **2**. The applied field is 20 Oe. The figure also shows the d*FCM*/d*T* derivative. Bottom: In-phase, χ_M', and out-of-phase, χ_M'', versus T curves for compound **2**. The vertical straightline corresponds to the extremum of d*FCM*/d*T*.

increase at 24 K, then reaches a plateau at about 3900 emu Oe mol^{-1} below 20 K. The derivative curve, dFCM/dT, presents an extremum at 22.8 K, corresponding to the critical temperature, T_c. The REM vanishes above $T_c =$ 22.8 K. The χ_M' curve is very similar to the FCM curve with a rapid increase between 24 and 21.5 K, and below this temperature a slight decrease. The χ_M'' curve becomes non-zero below 23.5 K, increases in an abrupt fashion as T is lowered down to 21.5 K, and then increases slightly. χ_M' and χ_M'' show no peak.

The field dependence of the magnetization for **2** is very similar to that observed for $[(Merad)_2Mn_2\{Cu(opba)\}_3(DMSO)_2]\cdot 2H_2O$.[37] At 10 K and under 50 kOe the magnetization value is 6.43 Nβ (Bohr magneton per mole). The hysteresis loop for **2** shows a coercitive field smaller than 10 Oe. This compound is a soft magnet.

Compound ***3***: The same magnetic experiments were performed for compound **3** as for compound **2**. The temperature dependence of $\chi_M T$ is shown in Figure 6. At room temperature $\chi_M T$ is equal to 6.93 emu K mol^{-1}, which is slightly lower than expected for isolated spin carriers. Then $\chi_M T$ decreases smoothly as the temperature is lowered, reaches a rounded minimum around 75 K, and increases very abruptly at lower temperature before reaching a maximum around 30 K. This $\chi_M T$ versus T curve reveals again antiferromagnetic interactions between noncompensating spin carriers, that is, a ferrimagnetic regime.

Figure 8 shows the FCM, REM (top), χ_M' and χ_M'' (bottom) versus T curves. The FCM curve shows a rapid increase below 38 K, and reaches a plateau at 3500 emu Oe mol^{-1} below 28 K. The derivative of this FCM curve has an extremum at 36.2 K, while the REM vanishes at a slightly higher temperature, 37.2 K. The χ_M' and χ_M'' curves have peaklike shapes, with

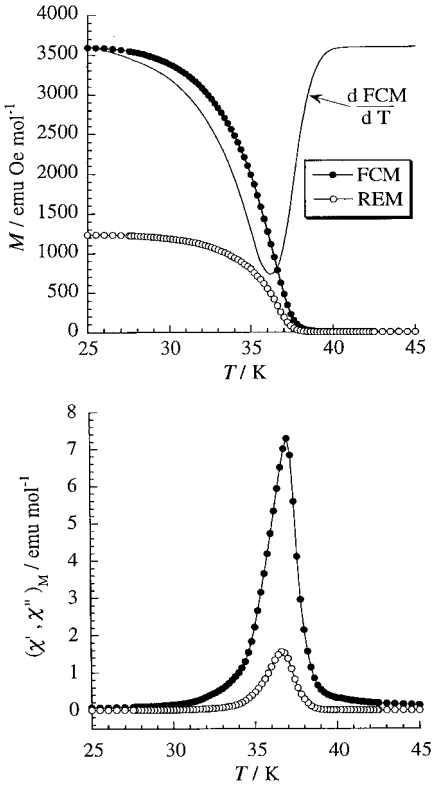

Figure 8. Top: FCM and REM versus T curves for compound **3**. The applied field is 20 Oe. The figure also shows the d*FCM*/d*T* derivative. Bottom: In-phase, χ_M', and out-of-phase, χ_M'', versus T curves for compound **3**. The vertical straightline corresponds to the extremum of d*FCM*/d*T*.

0947-6539/99/0505-1490 $ 17.50+.50/0 *Chem. Eur. J.* **1999**, *5*, No. 5

maximum values at 37 K and 36.7 K, respectively. It is worthwhile to notice that the maximum of χ_M' occurs at a temperature that is very close to that where the REM vanishes. This temperature, 37 K, may be considered as the critical temperature of the compound.

The most important feature for compound **3** is the field dependence of the magnetization. Figure 9 shows the hysteresis loop at 6 K for two different samples consisting of crystals of different average size. The black dots were

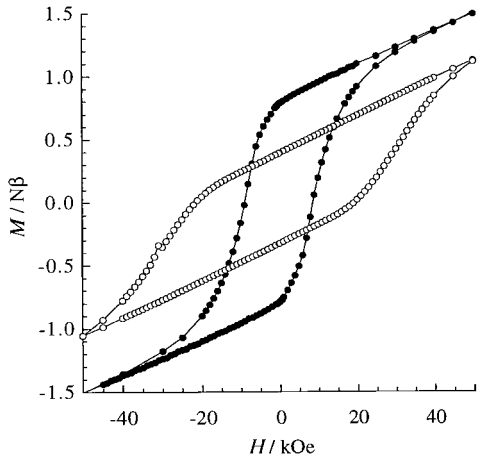

Figure 9. Field dependences of the magnetization for two samples of compound **3**: (●) the largest crystals; (○) the smallest crystals.

obtained with the largest crystals; the coercive field was found to be 8.5 kOe; the white dots were obtained with crystals whose volume is approximately 50 times smaller, and the coercive field appears to be of the order of 24 kOe. Let us notice, however, that for this latter sample the saturation magnetization is not reached under 50 kOe, so that the hysteresis loop is not measured accurately with our magnetometer, and the coercive field might be even larger than 24 kOe. An apparatus working at higher fields should be utilized. With crystals of intermediate size a coercive field of about 16 kOe was obtained. We have already discussed the origin of the coercivity of magnets, in particular of molecule-based magnets.[34, 39] This coercivity depends on both chemical and structural factors. These two aspects are illustrated here. The high-spin Co^{2+} ion in a distorted octahedral environment has a strong magnetic anisotropy, while the Mn^{2+} ion in the same environment is almost isotropic. This chemical difference between compounds **2** and **3** explains why the latter is much more coercive than the former. However, the coercive field of the hard molecule-based magnet **3** also depends on structural factors such as particle size and shape.[40]

*Mixed Compounds (**4** – **x**)*: The mixed compounds **4** – ***x*** were synthesized with a view to fine tuning the magnetic properties. The limits $x = 0$ and 1 correspond to pure compounds **2** and **3**, respectively. Four crystalline samples were obtained, namely **4-0.26**, **4** – **0.52**, **4** – **0.79**, and **4** – **0.90**. The $\chi_M T$ versus T curve for these four compounds shows a minimum that is characteristic of the ferrimagnetic regime. The larger x is, the lower the temperature of this minimum. A typical example, that of compound **4** – **0.52**, is shown in Figure 6. The shapes of ac magnetic responses are very similar to those obtained for **3** with the peaks of χ_M' and χ_M'' depending on the composition defined by x. The critical temperatures for these mixed compounds were estimated as the inflexion points of the χ_M' versus T curves. The variation of T_c as a function of x is almost linear, as shown in Figure 10. This figure also gives the

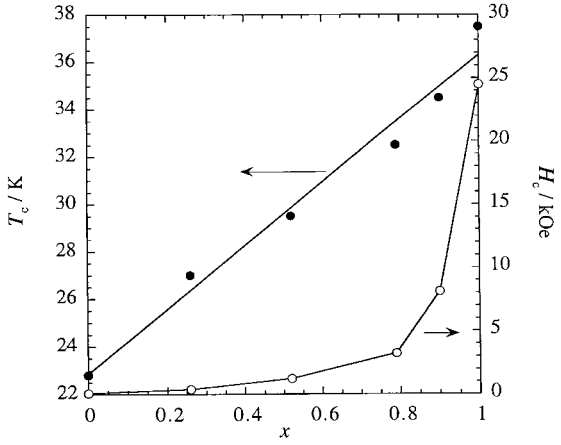

Figure 10. Variation of the critical temperature, T_c, and of the coercive field, H_c, as a function of x for the mixed compounds $(Etrad)_2Mn_{2-2x}Co_{2x}Cu_3$ (**4** – ***x***). The straight line for T_c corresponds to a linear regression of the experimental data. The line for H_c is just an eye guide.

variation of the coercive field, H_c, at 6 K as a function of x for samples prepared in a similar way, and consisting of crystals of similar size. H_c does not vary linearly with x, but with a slope increasing rapidly as x increases. The profile of this $H_c = f(x)$ curve may be easily understood. As a matter of fact, we write Equations (3) and (4),[40, 41] in which $K(x)$ and $M_s(x)$ are the anisotropy constant and the magnetic density (per unit of volume) for the mixed compound **4** – ***x***; K_M and M_M (M = Mn or Co) are the anisotropy contants and magnetic densities for the pure compounds **2** and **3**, respectively. K_{Mn} may be considered as being negligibly small as compared to K_{Co}. Assuming that the particles are spherical and monodomain results in Equations (5) and (6), in which with $\rho = M_{Mn}/M_{Co}$.[37]

$$K(x) = (1-x)K_{Mn} + xK_{Co} \quad (3)$$

$$M_S(x) = (1-x)M_{Mn} + xM_{Co} \quad (4)$$

$$H_c(x) = 0.96\ \mathrm{K}(x)/M_S(x) \quad (5)$$

$$H_c(x) = H_c(x=1)\,\frac{x}{x(1-\rho)+\rho} \quad (6)$$

Even if M_{Co} is difficult to evaluate owing to the first-order angular momentum for the Co^{2+} ion in octahedral environment, ρ is certainly larger than the unity; as a matter of fact, Mn^{2+} is more magnetic than Co^{2+}. It follows that the $H_c = f(x)$ curve for the mixed compounds **4** – ***x*** is expected to exhibit the curvature experimentally observed (see Figure 10).

Discussion

Let us begin this discussion by a few remarks concerning both the synthesis and the crystal growing of compounds **2** and **3**. The syntheses are exceptionally critical. First, the purity of the precursor **1** is crucial. Furthermore, the experimental conditions leading to the magnets **2** and **3** need to be very carefully and precisely adjusted. In addition to these compounds **2** and **3**, the reactions may lead to chain compounds of formula $MCu(opba)\cdot S$ and uncharacterized two-dimensional compounds in which the networks are probably not interlocked. The most critical parameters, in addition to the purity of **1**, are the concentrations and the temperature. The syntheses were carried out in a temperature controlled room. Finally, it must be stressed that, although **2** and **3** are isomorphous, their syntheses as well as the methods of crystal growing are quite different.

Let us now focus on the physical properties. One of the most important aspects of this work concerns the comparison between soft (**2**) and hard (**3**) molecule-based magnets. The two compounds are isomorphous, and the only difference between them is the replacement of Mn^{2+} in **2** by Co^{2+} in **3**. Both ions are in distorted octahedral surroundings. Mn^{2+} has a $^6A_1$ local ground state, with a very weak local anisotropy. The zero-field splitting parameter in such a case is known to be of the order of 10^{-2} wavenumbers. Co^{2+} has a $^4T_1$ local ground state, and the combined effect of symmetry lowering and spin-orbit coupling gives rise to two low-lying Kramers doublets, which can be separated by several tens of wavenumbers. Furthermore, the g tensor associated with the ground Kramers doublet is expected to be strongly anisotropic as well.[42] As a consequence of these differences between Mn^{2+} and Co^{2+}, the coercive field for **2** at 6 K is of the order of 10 Oe, and that of **3** at the same temperature of the order of 10^4 Oe.

This work also points out that the coercivity of a magnet is not an intrinsic property, but strongly depends on structural factors like particle shape and size, and homogeneity of the material. Of course, such a situation was well documented for magnetic alloys and ionic lattices, but not proved yet for molecule-based materials. Actually, the size factor seems to be much more important than the shape factor. As a matter of fact, the largest coercive field due to shape properties is expected for needle-shaped monodomain particles. In such a case, the coercive field is equal to $0.96\pi M_s^2$ where M_S is the magnetic density.[40] For molecule-based magnets, M_S is obviously very weak, compared with metallic magnets, so that the shape of the particles should not play a key role. Three samples of **3** were investigated, differing in the average size of the crystals, and the coercive field at the same temperature (6 K) varies from 8.5 kOe for the largest crystals to about 24 kOe for the smallest ones.

The differences between **2** and **3** are not limited to the shapes of the magnetic hysteresis loops. The differences of ac magnetic responses also deserve to be commented (see bottom of Figures 7 and 8). Two features are more particularly significant, namely:

1) In the magnetically-ordered state the ratio χ_M''/χ_M' at any temperature is much larger for **3** (ca. 20%) than for **2** (ca 1.5%). In Figure 8 χ_M' and χ_M'' are plotted with the same vertical scale, while in Figure 7 it was necessary to use two scales; otherwise, the out-of-phase response would not be visible. The magnetic anisotropy in the hard magnet enhances the relaxation phenomena, which in turn increases the out-of-phase response, χ_M''.
2) χ_M' and χ_M'' present a plateau below T_c for **2**, and have a peaklike shape for **3**. In other terms the FCM curve and the χ_M' curve have the same profile for the soft magnet **2**. It is not the case anymore for the hard magnet **3**.

This situation may be easily explained. For the soft magnet FCM and zero-field-cooled magnetization (ZFCM) curves are almost identical. It follows that $\chi_M' = dM/dH$ in zero field varies as the FCM measured in low field, 20 Oe in this work. For the hard magnet FCM and ZFCM curves are very different. In particular, the ZFCM is very weak at low temperature, much below T_c, and presents a maximum at a temperature just below T_c. It follows that χ_M' should exhibit a peak, as observed in Figure 8.

Another important aspect of our work concerns the mixed compounds $\mathbf{4}-\boldsymbol{x}$. The critical temperature varies almost linearly as a function of x. This is not the case for the coercive field. For samples consisting of particles of approximately the same size the slope of the $H_c = f(x)$ plot increases as x increases.

To finish this discussion we would like to address briefly the problem of the determination of T_c from dc and ac magnetic data. In the dc mode two criteria are more frequently used, namely the inflexion point of the FCM curve, and the vanishing of the REM curve. For the soft magnet **2**, these two approaches lead to the same result, $T_c = 22.8$ K. On the other hand, there is a difference of 1 K between the two determinations for the hard magnet **3** (36.2 K and 37.2 K). In the ac mode some authors have suggested the determination of T_c as the maximum of χ_M', or alternatively of χ_M''. Both approaches are quite questionable. First, χ_M' and/or χ_M'' may not display a maximum; this is the case of χ_M'' for **2**. Secondly, the profiles of the χ_M' and χ_M'' versus T curves are governed by complicated relaxation phenomena which are not directly related to T_c. Perhaps, the most erroneous approach is to determine T_c as the maximum of χ_M'', if any. It is probably a bit less uncorrect to say that T_c is close to the temperature where χ_M'' is not strictly zero, and slightly below. To sum up this discussion concerning T_c, we can say that the order parameter of the long-range magnetic ordering is the spontaneous magnetization, so that it is correct to determine T_c as the temperature at which the REM vanishes. However, it is not always easy to obtain the genuine REM curve. In particular, this requires us to work in strictly zero field. For a soft magnet, T_c also corresponds to the extremum of the derivative $dFCM/dT$. This is not strictly true anymore for a coercive magnet.

Conclusion

The molecule-based magnets are still a rather new class of materials. It was already well established that as more common metallic or ionic magnets they exhibit a spontaneous magnetization below a certain critical temperature. This

0947-6539/99/0505-1492 $ 17.50+.50/0 *Chem. Eur. J.* **1999**, *5*, No. 5

critical temperature may be found above room temperature.[28] This paper confirms that they may also behave as hard magnets with strong coercive fields. $[(Etrad)_2Co_2\{Cu(opba)\}_3(DMSO)_{1.5}]\cdot 0.25H_2O$ (**3**) exhibits one of the strongest coercive fields reported so far for molecule-based materials. Very recently Kurmoo and co-workers also reported on a very hard magnet synthesized from molecular precursors.[43] The possibility to design molecule-based materials displaying wide magnetic-hysteresis loops was not obvious, at least for us. Actually, some time ago, we thought that the softness of the molecular state would prevent us from synthesizing very coercive magnets. We were not right; there is no contradiction between soft lattices and hard magnets. The key factor of the coercivity for compound **3** is the presence of the very anisotropic Co^{2+} spin carrier. This factor, however, is not the only one. The Co^{2+} containing two-dimensional magnets of formula $[(cat)_2Co_2\{Cu(opba)\}_3]\cdot S$ display coercive fields at 5 K weaker than 5 kOe. The three-dimensional character of **3** resulting from the interlocking of two quasi-perpendicular graphitelike networks contributes to the coercivity.

Critical temperatures and coercive fields are physical characteristics common to all sorts of magnets. The presence of three different kinds of spin carriers in **2** and **3** along with the chicken-wire netting topology are more specific to the molecular state. We are presently studying the physical properties related to the molecular nature of the compounds and will report on the ferromagnetic (ferrimagnetic) resonance for compound **2** in the near future.

Experimental Section

Syntheses: The radical 2-(pyridine-4-yl)-4,4,5,5-tetramethylimidazoline-1-oxyl-3-oxide, abbreviated as rad,[36, 37, 44] the ligand opba, and the tetrabutylammonium salt of the Cu^{2+} precursor, $[(NBu_4)_2Cu(opba)]$,[11, 37] were prepared as already described.

$Etrad^+I^-$: A solution of rad (0.43 g, 1.8×10^{-3} mol) and iodomethane (2 mL, 3.9 g, 2.5×10^{-2} mol) in tetrahydrofuran (1 mL) was maintained under stirring for 72 hours at room temperature. The resulting green precipitate was collected by filtration, washed with THF, and dried under vacuum. Yield: 0.61 g (86%); $C_{14}H_{21}N_3O_2I$ (390.24): calcd C 43.08, H 5.44, N 10.77; found C 42.35, H 5.94, N 10.40.

$[(Etrad)_2Cu(opba)]\cdot CH_3CN\cdot H_2O$ (1): $[(NBu_4)_2Cu(opba)]$ (0.94 g, 1.2×10^{-3} mol) was added into a solution of $Etrad^+I^-$ (1 g, 2.6×10^{-3} mol) in dichloromethane (35 mL) under vigorous stirring. After 20 min, a brown polycristalline powder precipitated, which was filtered off, washed with CH_2Cl_2, and dried under vacuum. Well-shaped brown single crystals of **1** suitable for X-ray structure determination were obtained from a CH_3CN solution. Yield: 0.97 g (90%); $C_{40}H_{51}N_9O_{11}Cu$ (897.44): calcd C 53.53, H 5.73, N 14.05, Cu 7.08; found C 53.75, H 5.70, N 13.40, Cu 7.14.

$[(Etrad)_2Mn_2\{Cu(opba)\}_3(DMSO)_{3.5}]\cdot 3H_2O$ (2): A solution of $MnCl_2\cdot 4H_2O$ (0.0107 g, 6×10^{-5} mol) in DMSO (3 mL) was added to a solution of **1** (0.30 g, 3.34×10^{-4} mol) in DMSO (6 mL). The mixture was stirred at 21 °C for 10 min. The color slowly turned to green. The compound was cristallized as follows: small aliquots of the mother-liquor were placed into Petri dishes that were then covered with a parafilm and allowed to stand. The first crystals appeared within a few hours, were collected after 5 days of standing, and washed with DMSO. $C_{65}H_{81}N_{12}O_{28.5}S_{3.5}Mn_2Cu_3$ (1899.70): calcd C 41.11, H 4.30, N 8.85, S 5.91, Cu 10.04, Mn 5.78; found C 41.32, H 4.30, N 8.95, S 5.57, Cu 9.06, Mn 5.05.

$[(Etrad)_2Co_2\{Cu(opba)\}_3(DMSO)_4]\cdot 5.5H_2O$ (3): A solution of $CoCl_2\cdot 6H_2O$ (0.025 g, 1.05×10^{-4} mol) in DMSO (4 mL) was added to a solution of **1** (0.125 g, 1.39×10^{-4} mol) in DMSO (11 mL). The solution was poured into a beaker and allowed to stand at 21 °C. After 20 days crystals suitable for X-Ray analysis were separated and washed with DMSO. The size of the crystals depends upon the period of standing. For magnetic measurements, several samples with different crystal sizes were isolated. $C_{66}H_{89}N_{12}O_{31.5}S_4Co_2Cu_3$ (1991.25): calcd C 39.81, H 4.51, N 8.44, S 6.44, Cu 9.57, Co 5.92; found C 39.72, H 4.20, N 8.33, S 6.27, Cu 10.00, Co 5.28.

$[(Etrad)_2Mn_{2-2x}Co_{2x}\{Cu(opba)\}_3(DMSO)_y]\cdot zH_2O$ ($4-x$): A solution of **1** (0.3 g, 3.35×10^{-4} mol) in DMSO (4.8 mL) was added to a solution containing a mixture of $CoCl_2\cdot 6H_2O$ and $MnCl_2\cdot 4H_2O$ in DMSO (1.3 mL) at 21 °C. The product was isolated by centrifugation, washed with DMSO and dried under vacuum. Four samples were isolated with different compositions and standing days, namely: (**4 – 0.26**): 22.5 mg of $CoCl_2\cdot 6H_2O$ and 67.5 mg of $MnCl_2\cdot 4H_2O$, 20 standing days; (**4 – 0.52**): 45 mg of $CoCl_2\cdot 6H_2O$ and 45 mg of $MnCl_2\cdot 4H_2O$, 28 standing days; (**4 – 0.79**): 72 mg of $CoCl_2\cdot 6H_2O$ and 18 mg of $MnCl_2\cdot 4H_2O$, 40 standing days; (**4 – 0.90**): 81 mg of $CoCl_2\cdot 6H_2O$ and 9 mg of $MnCl_2\cdot 4H_2O$, 40 standing days; (**4 – 0.26**): $C_{69}H_{91}N_{12}O_{29.5}S_{5.5}Mn_{1.48}Co_{0.52}Cu_3$ (2039.50): calcd C 40.64, H 4.50, N 8.24, S 8.65, Cu 9.35, Mn 3.99, Co 1.50; found: C 40.05, H 4.39, N 8.27, S 8.25, Cu 9.33, Mn 3.99, Co 1.37; (**4 – 0.52**): $C_{67}H_{89}N_{12}O_{30.5}S_{4.5}Mn_{0.96}Co_{1.04}Cu_3$ (1999.47): calcd C 40.25, H 4.49, N 8.41, S 7.22, Cu 9.53, Mn 2.64, Co 3.05, found: C 40.55, H 4.41, N 8.48, S 7.08, Cu 9.51, Mn 2.63, Co 2.82; (**4 – 0.79**): $C_{66}H_{86}N_{12}O_{30}S_4Mn_{0.41}Co_{1.59}Cu_3$ (1962.60): calcd C 40.39, H 4.42, N 8.56, S 6.53, Cu 9.71, Mn 1.15, Co 4.77; found C 40.65, H 4.37, N 8.86, S 6.01, Cu 9.15, Mn 1.08, Co 4.89; (**4 – 0.90**): $C_{65}H_{83}N_{12}O_{29.5}S_{3.5}Mn_{0.2}Co_{1.8}Cu_3$ (1924.37): calcd C 40.57, H 4.35, N 8.73, S 5.83, Cu 9.91, Mn 0.57, Co 5.51; found C 40.54, H 4.34, N 8.89, S 5.26, Cu 9.54, Mn 0.54, Co 4.94. All metal analyses were carried out by absorption spectroscopy.

We will note that the chemical analyses of compounds **2** and **3** revealed the presence of more water and DMSO molecules than detected by X-ray diffraction. Most likely, these additional solvent molecules are strongly disordered in the tunnels limited by the interlocked perpendicular layers. The magnetic data have been interpreted by using the molecular weights deduced from the chemical analyses.

Crystallographic data collection and structure determination: Data were collected with a Enraf-Nonius CAD4 diffractometer for compound **1**, and a Siemens SMART diffractometer for compounds **2** and **3**. The data reduction was performed with MOLEN[45] (for **1**), and structure solutions and refinements for the three compounds were carried out with the programs SHELXS-86[46] and SHELXL-93.[47] The small size and the instability of the crystals along with the complexity of the structures of **2**–**3** made the structure refinement very difficult. Furthermore, disorder and high thermal motion were observed for the DMSO and water molecules. Consequently, the values of the agreement factor R for **2** and **3** are rather high. The crystal data are summarized in Table 3. Crystallographic data (excluding structure factors) for the structures reported in this paper have been deposited with the Cambridge Crystallographic Data Centre as supplementary publication no. CCDC-103083, 103084, and 103085. Copies of the data can be obtained free of charge on application to CCDC, 12 Union Road, Cambridge CB2 1EZ, UK (fax: (+44) 1223-336-033; e-mail: deposit@ccdc.cam.ac.uk).

Magnetic measurements: These were carried out with a Quantum Design MPMS-5S SQUID magnetometer, working in both the dc and ac modes between 2 and 300 K, and from 0 to 50 kOe. In the dc mode the field-cooled magnetizations (FCM) were measured upon cooling the sample within a field of 20 Oe. The remnant magnetizations (REM) were obtained as the differences between two curves, 1 and 2. Curve 1 was measured in cooling down the sample within the field and then warming up in a field equal to zero according to the indication of the apparatus. Curve 2 was measured in cooling down within this zero field. This procedure allowed us to eliminate the influence of the remnant field present in the superconducting wires. The raw susceptibility data were corrected of the core diamagnetism estimated as -530×10^{-6} emu mol^{-1} for **2** and **3**. On the other hand, the core diamagnetism was considered as one of the parameters to fit for compound **1** (see above).

Acknowledgment

H. O. Stumpf acknowledges the support from the Conselho Nacional de Desenvolvimento Científico e Tecnológico (CNPq), the Fundação de Amparo a Pesquisa no Estado de Minas Gerais (FAPEMIG), and the Coordenaçao de Aperfeiçoamento de Pessoal de Nível Superior (CAPES).

Table 3. Crystal data and structure refinement for compounds **1**–**3**.

	1	**2**	**3**
formula	$C_{40}H_{51}N_9O_{11}Cu$	$C_{59}H_{57.5}N_{12}O_{22.75}S_{0.5}Cu_3Mn_2$	$C_{61}H_{63.5}N_{12}O_{23.75}S_{1.5}Co_2Cu_3$
M_R	897.44	1615.20	1701.31
λ [Å]	0.71073	0.71073	0.71073
T [K]	293(2)	293(2)	293(2)
crystal system	Monoclinic	Monoclinic	Monoclinic
space group	$P\bar{1}$	Cc	Cc
a [Å]	11.999(3)	24.3033(7)	24.646(3)
b [Å]	12.947(4)	25.0251(4)	24.854(3)
c [Å]	14.94(2)	18.2807(5)	18.181(2)
α [°]	82.78(4)	90	90
β [°]	68.04(3)	130.6780(10)	131.506(2)
γ [°]	83.82(2)	90	90
V [Å^3]	2131(3)	8431.9(4)	8340.1(15)
Z	2	4	4
ρ_{calcd} [Mg m^{-3}]	1.399	1.272	1.355
$\mu(Mo_{K\alpha})$, [mm^{-1}]	0.582	1.116	1.252
$F(000)$	942	3290	3474
θ range [°]	1.48–26.95	1.37–23.35	1.37–30.65
index ranges	$0 \le h \le 15$	$-20 \le h \le 26$	$-32 \le h \le 33$
	$-15 \le k \le 15$	$-22 \le k \le 27$	$-33 \le k \le 35$
	$-17 \le l \le 18$	$-20 \le l \le 20$	$-23 \le l \le 25$
refelctions collected	4907	16517	29465
independent reflections	4907	10463 [$R_{int} = 0.1435$]	15772 [$R_{int} = 0.5293$]
refinement method		full-matrix least-squares on F^2	
data/restraints/parameters	4907/0/699	10463/41/773	15770/2/556
goodness-of-fit on F^2	1.103	1.215	0.918
final R indices [$I > 2\sigma(I)$]	$R1 = 0.0562$, $wR2 = 0.1370$	$R1 = 0.1232$, $wR2 = 0.2788$	$R1 = 0.1474$, $wR2 = 0.2573$
R indices (all data)	$R1 = 0.0898$, $wR2 = 0.1473$	$R1 = 0.3005$, $wR2 = 0.3363$	$R1 = 0.5390$, $wR2 = 0.4340$
largest diff. peak:hole, [e Å^{-3}]	0.335/−0.522	1.152/−1.391	0.908/−0.653

This work was partly funded the the TMR Research Network ERB 4061 PL977-0197, entitled: Molecular Magnetism; from Materials toward Devices.

[1] J. S. Miller, J. C. Calabrese, A. J. Epstein, R. W. Bigelow, J. H. Zang, W. M. Reiff, *J. Chem. Soc. Chem. Commun.* **1986**, 1026.
[2] J. S. Miller, J. C. Calabrese, H. Rommelman, S. R. Chittipedi, J. H. Zang, W. M. Reiff, A. J. Epstein, *J. Am. Chem. Soc.* **1987**, *109*, 769.
[3] Y. Pei, M. Verdaguer, O. Kahn, J. Sletten, J.-P. Renard, *J. Am. Chem. Soc.* **1986**, *108*, 428.
[4] O. Kahn, Y. Pei, M. Verdaguer, J.-P. Renard, J. Sletten, *J. Am. Chem. Soc.* **1988**, *110*, 782.
[5] J. S. Miller, A. J. Epstein, *Angew. Chem.* **1994**, *106*, 399; *Angew. Chem. Int. Ed. Engl.* **1994**, *33*, 385.
[6] O. Kahn, *Molecular Magnetism*, VCH, New York, **1993**.
[7] O. Kahn, *Adv. Inorg. Chem*. **1995**, *43*, 179.
[8] Y. Nakazawa, M. Tamura, N. Shirakawa, D. Shiomi, M. Takahashi, M. Kinoshita, M. Ishikawa, *Phys. Rev.* **1992**, *B46*, 8906.
[9] R. Chiarelli, M. A. Nowak, A. Rassat, J.-L. Tholence, *Nature* **1993**, *363*, 147.
[10] D. Gatteschi, *Adv. Mater.* **1994**, *6*, 635.
[11] H. O. Stumpf, Y. Pei, O. Kahn, J. Sletten, J.-P. Renard, *J. Am. Chem. Soc.* **1993**, *115*, 6738.
[12] H. Tamaki, Z. J. Zhong, N. Matsumoto, S. Kida, S. Koikawa, S. Achiwa, Y. Hashimoto, H. Okawa, *J. Am. Chem. Soc.* **1992**, *114*, 6974.
[13] S. Decurtins, H. W. Schmalle, H. R. Oswald, A. Linden, J. Ensling, P. Gütlich, A. Hauser, *Inorg. Chim. Acta* **1994**, *216*, 65.
[14] M. Ohba, N. Maruono, H. Okawa, *J. Am. Chem. Soc.* **1994**, *116*, 11566.
[15] J. Larionova, B. Mombelli, J. Sanchiz, O. Kahn, *Inorg. Chem.* **1998**, *37*, 679–684.
[16] J. S. Miller, J. C. Calabrese, A. D. Dixon, A. J. Epstein, R. W. Bigelow, J. H. Zhang, W. M. Reiff, *J. Am. Chem. Soc.* **1987**, *109*, 769.
[17] W. E. Broderick, J. A. Thompson, E. P. Day, B. M. Hoffman, *Science* **1990**, *249*, 410.
[18] G. T. Yee, J. M. Manriquez, D. A. Dixon, R. S. McLean, D. M. Groski, R. B. Flippen, K. S. Narayan, A. J. Epstein, J. S. Miller, *Adv. Mater.* **1991**, *3*, 309.
[19] W. E. Broderick, B. M. Hoffman, *J. Am. Chem. Soc.* **1991**, *113*, 6334.
[20] D. M. Eichhorn, D. C. Skee, W. E. Broderick, B. M. Hoffman, *Inorg. Chem.* **1993**, *32*, 491.
[21] J. S. Miller, J. C. Calabrese, R. S. McLean, A. J. Epstein, *Adv. Mater.* **1992**, *4*, 498.
[22] K. Inoue, H. Iwamura, *J. Am. Chem. Soc.* **1994**, *116*, 3173.
[23] A. Caneschi, D. Gatteschi, R. Sessoli, P. Rey, *Acc. Chem. Res.* **1989**, *22*, 392.
[24] K. Inoue, T. Hayamizu, H. Iwamura, D. Hashizume, Y. Ohashi, *J. Am. Chem. Soc.* **1996**, *118*, 1803.
[25] H. Iwamura, K. Inoue, N. Koga, *New J. Chem.* **1998**, *10*, 201.
[26] T. Mallah, S. Thiebaut, M. Verdaguer, P. Veillet, *Science* **1993**, *262*, 1554.
[27] W. R. Entley, G. S. Girolami, *Science* **1995**, *268*, 397.
[28] S. Ferlay, T. Mallah, R. Ouahès, P. Veillet, M. Verdaguer, *Nature* **1995**, *378*, 701.
[29] J. Larionova, J. Sanchiz, S. Gohlen, L. Ouahab, O. Kahn, *Chem. Commun.* **1998**, 953.
[30] S. Descurtins, H. W. Schmalle, P. Schneuwly, H. R. Oswald, *Inorg. Chem.* **1993**, *32*, 1888.
[31] S. Descurtins, H. W. Schmalle, P. Schneuwly, J. Ensling, P. Gütlich, *J. Am. Chem. Soc.* **1994**, *116*, 9521.
[32] S. Descurtins, H. W. Schmalle, H. R. Oswald, A. Linden, J. Ensling, P. Gütlich, *Inorg. Chim. Acta* **1994**, *216*, 65.
[33] L. O. Atovmyan, G. V. Shilov, R. N. Lyubovskaya, E. Zhilyaeva, N. S. Ovanesyan, S. I. Pirumova, I. G. Gusakovskya, Y. G. Morozov, *JETP Lett.* **1993**, *58* , 766.
[34] C. Mathonière, C. J. Nuttall, S. Carling, P. Day, *Inorg. Chem.* **1996**, *35*, 1201.
[35] O. Cador, D. Price, J. Larionova, C. Mathonière, O. Kahn, J. V. Yakhmi, *J. Mater. Chem.* **1997**, *7* , 1263.
[36] H. O. Stumpf, L. Ouahab, Y. Pei, D. Grandjean, O. Kahn, *Science* **1993**, *261*, 447.
[37] H. O. Stumpf, L. Ouahab, Y. Pei, P. Bergerat, O. Kahn, *J. Am. Chem. Soc.* **1994**, *116*, 3866.
[38] S. R. Batten, R. Robson, *Angew. Chem.* **1998**, *110*, 1558; *Angew. Chem. Int. Ed.* **1998**, *37*, 1460.

0947-6539/99/0505-1494 $ 17.50+.50/0 *Chem. Eur. J.* **1999**, *5*, No. 5

[39] H. O. Stumpf, Y. Pei, C. Michaut, O. Kahn, J.-P. Renard, L. Ouahab, *Chem. Mater.* **1994**, *6*, 257.
[40] A. Herpin, *Théorie du Magnétisme*, Presses Universitaires de France, Paris, **1968**.
[41] C. Kittel, *Introduction to Solid State Physics*, Wiley, New York, **1976**.
[42] A. Abragam, B. Bleaney, *Electron Paramagnetic Resonance of Transition Ions*, Dover, New York, **1970**.
[43] M. Kurmoo, C. J. Kepert, *Mol. Cryst. Liq. Cryst.* in press.
[44] E. F. Ulman, J. H. Osiecki, D. G. B. Boocock, R. Darcy, *J. Am. Chem. Soc.* **1972**, *94*, 7049.
[45] *MOLEN*, Enraf-Nonius, Delft, The Netherlands, **1990**.
[46] G. M. Sheldrick, *SHELXS-86: Program for the Solution of Crystal Structure*, University of Göttingen (Germany), **1986**.
[47] G. M. Sheldrick, *SHELXL-93: Program for the Refinement of Crystal Structure*, University of Göttingen (Germany), **1993**.

Received: September 28, 1998 [F1364]